

amount of the buffer pair was dissolved in D<sub>2</sub>O to produce the equivalent.<sup>3b,c</sup> Mixtures of H<sub>2</sub>O-D<sub>2</sub>O (L<sub>2</sub>O) were prepared by volumetrically combining these solutions. Account was taken in computing final values of  $n$  of differences in the density at 25 °C between H<sub>2</sub>O ( $d = 0.997$  g/cm<sup>3</sup>) and D<sub>2</sub>O ( $d = 1.1044$  g/cm<sup>3</sup>),<sup>19</sup> as well as isotopic dilution of the L<sub>2</sub>O solutions by protons released by the buffer salt and additions of enzyme and substrate in H<sub>2</sub>O. The pH of the buffer in H<sub>2</sub>O was determined to within  $\pm 0.01$  unit on an Orion Model 701 A digital pH meter equipped with a Ross combination electrode.

**Kinetics.** Kinetics experiments were carried out by adding 0.1 mL of substrate solution followed by 0.1 mL of RNase solution (both in the Tris buffer, H<sub>2</sub>O) to 3 mL of buffer in a cuvette in the thermostated cell compartment of a Variant Cary Model 219 spectrophotometer. Concentrations of the enzyme and substrate in the cuvette were approximately 6  $\mu$ M and 0.33 mM, respectively. The absorbance increase owing to the hydrolysis of cCMP was continuously recorded at 284 nm.<sup>20</sup> In preliminary experiments, plots of  $\log(A_\infty - A_t)$  vs. time yielded straight lines through 90% reaction. For the experiments reported here, a Bascom-Turner data center was used to acquire and store 2000 evenly spaced voltages related to the absorbance increases through 9-10 half-lives. The stored data were treated according to the Guggenheim method to obtain pseudo-first-order rate coefficients  $k_{\text{obsd}}$ , which were divided by the RNase concentration to yield  $k_e$ . The Guggenheim treatment uti-

lized data from at least 3 half-lives; the constant difference between readings taken at a series of times and a series of times later was selected to be approximately 2 half-lives. The mean value of  $k_{E,0}$  taken from four proton inventories was  $1180 \pm 50$  M<sup>-1</sup> s<sup>-1</sup>, in reasonably good agreement with the value of 1380 M<sup>-1</sup> s<sup>-1</sup> calculated from the expression

$$k_{E,0} = k_{\text{im}} / (1 + H_a/K_a + K_b/H_b)$$

where  $k_{\text{im}} = 7540$  M<sup>-1</sup> s<sup>-1</sup>,  $\text{p}K_a = 5.4$ , and  $\text{p}K_b = 6.8$  (25 °C, 0.1 M NaCl + 0.1 M Tris-acetate).<sup>21</sup>

A few five-point proton inventories were conducted in the usual way except the enzyme was dissolved in buffer constituted in D<sub>2</sub>O rather than in H<sub>2</sub>O. The values of  $k_{E,n}$ , the partial KSIEs, and the shapes of the proton inventory curves thus obtained were identical within the precision of the measurements with those found when the RNase was dissolved in the buffer constituted in H<sub>2</sub>O. This suggests that slow exchange of solvent deuterons with protons of the protein during the time required to prepare the enzyme solution and conduct a complete proton inventory (8-10 h) does not produce conformational or other changes that might surreptitiously confound the reported results.

**Acknowledgment.** This research was supported by National Institutes of Health Grant GM 32397. We thank Dr. Ross L. Stein for assistance with the curve-fitting procedure.

**Registry No.** RNase, 9001-99-4; cCMP, 633-90-9; D<sub>2</sub>, 7782-39-0; histidine, 71-00-1.

(19) Arnett, E. M.; McKelvey, D. R. In *Solvent-Solute Interactions*; Coetzee, J. F., Ritchie, D. D., Eds.; Marcell Dekker: New York, 1969; pp 392-394.

(20) Crook, E. M.; Mathias, A. P.; Rabin, B. R. *Biochem. J.* **1960**, *74*, 234-238.

(21) del Rosario, E. J.; Hammes, G. G. *Biochemistry* **1969**, *8*, 1884-1889.

## Low-Temperature Magnetic Circular Dichroism Studies of Native Laccase: Confirmation of a Trinuclear Copper Active Site

Darlene J. Spira-Solomon, Mark D. Allendorf, and Edward I. Solomon\*

Contribution from the Department of Chemistry, Stanford University, Stanford, California 94305. Received January 21, 1986

**Abstract:** Low-temperature magnetic circular dichroism (LTMCD), absorption, and EPR spectroscopies are used to determine the spectral features associated with the different types of copper in native laccase and to investigate N<sub>3</sub><sup>-</sup> and F<sup>-</sup> binding at this multicopper active site. This combination of techniques allows ligand field (d-d) and charge-transfer (CT) spectral features associated with the paramagnetic type 2 Cu(II) center to be differentiated from those of the antiferromagnetically coupled and therefore diamagnetic type 3 Cu(II) center. N<sub>3</sub><sup>-</sup> binding with  $K \sim 200$  M<sup>-1</sup> ("low-affinity") to fully oxidized native laccase generates LTMCD and absorption features at 485 nm, assigned to N<sub>3</sub><sup>-</sup> → type 2 Cu(II) CT, and an absorption feature at 400 nm with no corresponding LTMCD intensity, assigned to N<sub>3</sub><sup>-</sup> → type 3 (coupled) Cu(II) CT. This indicates that N<sub>3</sub><sup>-</sup> bridges between the type 2 and type 3 cupric centers. This type 2/type 3 bridging mode is strongly supported by spectral perturbations. The intensities of these two features decrease together with increasing pH. In addition, studies of the competitive binding of N<sub>3</sub><sup>-</sup> and F<sup>-</sup> show that the binding of a single F<sup>-</sup> to the type 2 Cu(II) causes both the 400-nm absorption and 485-nm LTMCD bands to decrease by similar amounts. These correlations eliminate the possibility that two different N<sub>3</sub><sup>-</sup>'s with similar binding constants bind separately to the type 2 and type 3 centers and strongly support a single bridging N<sub>3</sub><sup>-</sup>. A second N<sub>3</sub><sup>-</sup> binds with  $K \geq 10^4$  M<sup>-1</sup> ("high-affinity") and generates LTMCD and absorption features at 510 and 450 nm that are associated with N<sub>3</sub><sup>-</sup> binding to the type 2 Cu(II) in a fraction (~25%) of the laccase molecules that contain a reduced type 3 copper center. Maximum intensity of these features is obtained with <1.0 protein equiv of N<sub>3</sub><sup>-</sup> ([protein]  $\approx$  1.0 mM), and addition of small amounts of N<sub>3</sub><sup>-</sup> to peroxide-oxidized laccase results in significantly decreased intensities of the 510- and 450-nm features. EPR studies of F<sup>-</sup> binding to oxidized native laccase in 50% glycerol/phosphate buffer solutions show a clear superhyperfine doublet of the type 2 Cu(II) signal, indicating that one F<sup>-</sup> binds to the type 2 Cu(II). The results of the N<sub>3</sub><sup>-</sup>/F<sup>-</sup> competition studies show that this F<sup>-</sup> binds to the type 2 site at room and low temperatures. Ligand competition studies of high-affinity N<sub>3</sub><sup>-</sup> with F<sup>-</sup> indicate that F<sup>-</sup> binds to the type 2 Cu(II) only when the type 3 coppers are oxidized. Investigation of the LTMCD features of native and peroxide-oxidized laccase, and their pH dependence, enables specific LTMCD features to be associated with the oxidized type 1 and type 2 centers in the presence of both reduced and oxidized type 3 centers (which do not contribute to the LTMCD spectrum). Changes in the type 2 d-d bands upon type 3 reduction demonstrate that the geometry of the type 2 center is strongly affected by the oxidation state of the type 3 center. The dependence of N<sub>3</sub><sup>-</sup> and F<sup>-</sup> affinity for the type 2 Cu(II) upon the oxidation state of the type 3 copper further demonstrates the strong interaction between these copper centers in anion binding. Finally, the presence of a type 2-type 3 trinuclear copper active site that is capable of binding and bridging at least the small molecule N<sub>3</sub><sup>-</sup> suggests that a similar binding mode could contribute to the multielectron reduction of dioxygen to water at this site.

The multicopper oxidases,<sup>1,2</sup> laccase, ceruloplasmin, and ascorbate oxidase, catalyze the four-electron reduction of dioxygen

to water, with concomitant one-electron oxidations of substrate. The active site of laccase is the simplest of these enzymes, con-

taining four copper ions that have been classified<sup>1</sup> according to their EPR features: type 1 or blue ( $A_{\parallel} \leq 95 \times 10^{-4} \text{ cm}^{-1}$ ), type 2 or normal ( $A_{\parallel} > 140 \times 10^{-4} \text{ cm}^{-1}$ ), and type 3 or coupled binuclear, which is EPR nondetectable. The oxygen reactivity of the multicopper oxidases differs significantly from that of the hemocyanins<sup>3,4</sup> and tyrosinase,<sup>3,5</sup> which bind oxygen reversibly as peroxide, bridging the binuclear Cu(II) site with a  $\mu$ -1,2 coordination geometry.<sup>6</sup> Since laccase contains only one of each type of copper site (ceruloplasmin has five to seven copper ions and ascorbate oxidase six to eight)<sup>7</sup> it provides the optimum system for initial study of this difference in oxygen reactivity.

The coordination environment and reactivity of the type 3 site in *Rhus vernicifera* laccase has been probed through spectroscopic studies<sup>8</sup> of the type 2 Cu(II)-depleted (T2D) derivative,<sup>9</sup> which, as prepared, contains a reduced type 3 center in the presence of an oxidized type 1 copper center<sup>10,11</sup> (deoxy-T2D). The type 3 site in peroxide-oxidized T2D<sup>10,12</sup> (met-T2D) is similar to the active site of hemocyanin in that it contains two tetragonal, antiferromagnetically coupled Cu(II) ions in which the electron superexchange is mediated by a protonatable<sup>8</sup> endogenous bridge (OR<sup>-</sup>; R = Ph, H, alkyl). In contrast to deoxyhemocyanin, however, oxygen does not react with the binuclear Cu(I) site in deoxy-T2D laccase.<sup>8,11</sup> Our spectroscopic studies of anion binding to the T2D derivatives<sup>8</sup> further indicate that exogenous anions do not bridge the type 3 site in T2D but bind equatorially to one copper center. The inability of anions to bridge the type 3 coppers appears to be due to the presence of only one equatorial exchangeable position at the type 3 site and is likely related to the lack of oxygen reactivity of deoxy-T2D. Oxygen readily oxidizes fully reduced native laccase, however, and comparative anion binding studies of T2D and native laccase indicate that significant differences in exogenous ligand interactions exist between these two forms, pointing to an important role for the type 2 copper in the binding of small molecules to the multicopper active site.

In a preliminary report,<sup>13</sup> the interaction of exogenous ligands with the type 2 and type 3 centers in native laccase was probed by using low-temperature magnetic circular dichroism (LTMCD) spectroscopy. The binding of the exogenous ligand inhibitor, azide, produces intense absorption features in the visible/UV region that are assigned as ligand  $\rightarrow$  Cu(II) charge-transfer (CT) transitions. The magnetic ground state associated with an observed CT band may be determined by examining the temperature dependence of the corresponding MCD feature: magnetically degenerate ground states give rise to MCD features whose intensity is proportional to  $1/T$  for  $kT > g\beta H$  ( $C$  term), while MCD features arising from magnetically nondegenerate ground states are temperature independent. The two structural units in laccase capable of anion binding and thus of producing exogenous ligand  $\rightarrow$  Cu(II) CT features are the types 2 and 3 centers. These have different

magnetic ground states: the type 2 is magnetically degenerate ( $S = 1/2$ ) giving rise to a  $g_{av} \approx 2.2$  EPR signal, while the antiferromagnetically coupled Cu(II) pair of the type 3 site has a nondegenerate ground state with total spin  $S = 0$  (the  $S = 1$  level is not significantly populated for  $T \leq 300 \text{ K}$ , as  $|2J| > 550 \text{ cm}^{-1}$ ).<sup>14,15</sup> Thus, CT bands associated with anion binding to the type 2 center will give rise to temperature-dependent MCD bands, while CT bands associated with anion binding to the coupled type 3 center will be temperature independent. At very low temperatures ( $T \leq 10 \text{ K}$ ) the MCD features from the diamagnetic type 3 ground state will be 100–1000 times weaker than those from the paramagnetic type 2 center;<sup>16</sup> hence, the presence of a LTMCD feature corresponding to a CT band is a direct indication that the CT band is associated with the type 2 Cu(II). LTMCD and absorption studies of  $\text{N}_3^-$  binding together determined<sup>13</sup> that CT features from both the type 2 and the type 3 centers were produced that displayed the same behavior as a function of  $[\text{N}_3^-]$  and pH, suggesting that  $\text{N}_3^-$  bridges these two centers. In this paper we present new results from systematic LTMCD studies that strongly support this model, demonstrating that the type 2 and type 3 centers comprise a trinuclear copper cluster that is capable of binding anions (i.e., azide) in a bridging geometry between the type 2 and one of the type 3 Cu(II) centers.

In addition to azide, other exogenous ligands inhibit oxygen reduction by laccase.<sup>7a</sup> In particular, fluoride, as determined by EPR,<sup>17</sup> binds to the type 2 Cu(II) with an extremely high affinity ( $K > 10^4$  higher than for aqueous copper complexes)<sup>18</sup> and changes the redox properties of the type 3 site such that the type 2 and type 3 centers now undergo reduction at the same potential.<sup>19</sup> The present work further develops our original LTMCD studies of the native laccase active site, the results of which are briefly presented and used as a probe of  $\text{F}^-$  binding through its competition with  $\text{N}_3^-$ . As both the type 1 and type 2 centers are paramagnetic and contribute to the LTMCD spectrum, we first consider the LTMCD spectrum of native laccase in which transitions due to these sites are clearly distinguished; these features are found to be a function of the oxidation state of the type 3 copper, also indicating a strong interaction between the type 2 and type 3 copper centers.

## Experimental Section

Laccase was obtained from the acetone powder (1983–1985 crops) of the Japanese lacquer tree, *R. vernicifera* (Saito and Co., Osaka, Japan), and purified according to published procedures,<sup>20</sup> as modified in ref 8. We note that enzyme isolated from the 1983–1984 acetone powder was found after the final CMC-50 column to contain a low molecular weight heme impurity [absorption maximum at 408 nm; LTMCD maxima at 410(+) and 426(-) nm] that obscured the LTMCD features of laccase and was removed by G-75 chromatography.<sup>21</sup> Protein solutions were routinely concentrated to  $\sim 0.4 \text{ mM}$  by using an Amicon YM-10 membrane.

Samples for low-temperature absorption and MCD spectra were dialyzed into 50% (v/v) glycerol/0.2 M potassium phosphate buffer, which gives a high-quality glass at temperatures below 200 K. This dialysis further concentrated the sample to 0.8–1.0 mM, giving a 298 K absorption of  $\sim 1.0$  at 615 nm in a 1.5-mm path length. Concentrated aqueous anion solutions (usually 5  $\mu\text{L}$  in volume of an appropriate concentration) were added directly to 200–400- $\mu\text{L}$  aliquots of protein and allowed to equilibrate for 16–24 h (except in the case of fluoride, for which the samples were equilibrated for 36–48 h).

Peroxide-oxidized<sup>12</sup> native laccase was prepared by reaction of  $\sim 0.3$ – $0.4 \text{ mM}$  protein with 20–30 protein equiv of  $\text{H}_2\text{O}_2$ ; excess peroxide

(1) (a) Malkin, R.; Malmstrom, B. G. *Adv. Enzymol.* **1970**, *33*, 177. (b) Malmstrom, B. G.; Andreasson, L.-E.; Reinhammar, B. In *The Enzymes*; Boyer, P. D., Ed.; Academic: New York, 1975; Vol. XII.

(2) Fee, J. A. *Struct. Bonding (Berlin)* **1975**, *23*, 1–60.

(3) Solomon, E. I. In *Copper Proteins*; Spiro, T. G., Ed.; Wiley-Interscience: New York, 1981; Chapter 2.

(4) Himmelwright, R. S.; Eickman, N. C.; LuBien, C. D.; Solomon, E. I. *J. Am. Chem. Soc.* **1980**, *102*, 5378–5388.

(5) Himmelwright, R. S.; Eickman, N. C.; LuBien, C. D.; Lerch, K.; Solomon, E. I. *J. Am. Chem. Soc.* **1980**, *102*, 7339–7344.

(6) Eickman, N. C.; Himmelwright, R. S.; Solomon, E. I. *Proc. Natl. Acad. Sci. U.S.A.* **1979**, *76*, 2094–2098.

(7) (a) Reinhammar, B.; Malmstrom, B. G. In *Copper Proteins*; Spiro, T. G., Ed.; Wiley-Interscience: New York, 1980; Chapter 3. (b) Laurie, S. H.; Mohammed, E. S. *Coord. Chem. Rev.* **1980**, *33*, 279–312. (c) Marchesini, A.; Kroneck, P. M. H. *Eur. J. Biochem.* **1979**, *101*, 65–76.

(8) Spira-Solomon, D. J.; Solomon, E. I., paper submitted for publication.

(9) Graziani, M. T.; Morpurgo, L.; Rotilio, G.; Mondovi, B. *FEBS Lett.* **1976**, *70*, 87–90.

(10) LuBien, C. D.; Winkler, M. E.; Thamann, T. J.; Scott, R. A.; Co, M. S.; Hodgson, K. O.; Solomon, E. I. *J. Am. Chem. Soc.* **1981**, *103*, 7014–7016.

(11) Hahn, J. E.; Co, M. S.; Hodgson, K. O.; Spira, D. J.; Solomon, E. I. *Biochem. Biophys. Res. Commun.* **1983**, *112*, 737–745.

(12) Penner-Hahn, J. E.; Hedman, B.; Hodgson, K. O.; Spira, D. J.; Solomon, E. I. *Biochem. Biophys. Res. Commun.* **1984**, *119*, 567–574.

(13) Allendorf, M. D.; Spira, D. J.; Solomon, E. I. *Proc. Natl. Acad. Sci. U.S.A.* **1985**, *82*, 3063–3067.

(14) Solomon, E. I.; Dooley, D. M.; Wang, R. H.; Gray, H. B.; Cerdonio, M.; Mogno, F.; Romani, G. L. *J. Am. Chem. Soc.* **1976**, *98*, 1029–1031.

(15) Dooley, D. M.; Scott, R. A.; Ellinghaus, J.; Solomon, E. I.; Gray, H. B. *Proc. Natl. Acad. Sci. U.S.A.* **1978**, *75*, 3019–3022.

(16) Stephens, P. J. *Adv. Chem. Phys.* **1976**, *35*, 197–264.

(17) Branden, R.; Malmstrom, B. G.; Vanngard, T. *Eur. J. Biochem.* **1973**, *36*, 195–200.

(18) Winkler, M. E.; Spira, D. J.; LuBien, C. D.; Thamann, T. J.; Solomon, E. I. *Biochem. Biophys. Res. Commun.* **1982**, *107*, 727–734.

(19) Reinhammar, B. *Biochim. Biophys. Acta* **1972**, *275*, 245–259.

(20) (a) Reinhammar, B. *Biochim. Biophys. Acta* **1970**, *205*, 197–264. (b) Reinhammar, B.; Oda, Y. *J. Inorg. Biochem.* **1979**, *11*, 115–127.

(21) Fletcher, M.; Spira, D. J.; Solomon, E. I., unpublished results.

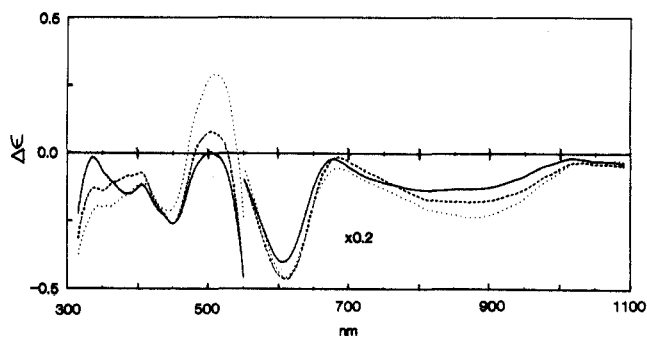


**Figure 1.** MCD spectra of native laccase at 4.8 K: (—) pH 7.0; (---) pH 6.0; (···) pH 4.6. [Protein] = 0.88 mM.

was removed by G-25 chromatography. The protein was then dialyzed into glycerol phosphate as above. Absorption spectra of the dialyzed protein routinely showed  $\geq 80\%$  retention of the peroxide oxidation observed before the G-25 and dialysis treatment.

Room-temperature absorption spectra of samples used for MCD spectroscopy were run in 2.0-mm quartz cells on either a Cary 14 or Cary 17 spectrometer. To obtain absorption and MCD spectra at low temperatures, protein samples were injected into a cell composed of two quartz disks ( $\sim 1$ -cm diameter) spaced by a 1.5-mm rubber gasket. Samples were mounted in this way either on an Air Products LTD-3-110 Heli-Tran liquid-helium transfer refrigerator (sample temperatures of 7–300 K) for absorption spectroscopy on a Cary 17 or on a sample rod for insertion into a superconducting magnet/cryostat for MCD spectroscopy.

The MCD spectrometer consists of a Jasco J500-C spectropolarimeter equipped with S20 and S1 photomultipliers and a 450-W xenon arc lamp, giving a spectral range of 200–1100 nm. The sample compartment was modified<sup>22</sup> to accommodate an Oxford Instruments Spectromag 4 superconducting magnet/cryostat, capable of producing fields up to 60 kG. This extended the light path to  $\sim 90$  cm from the J500-C to the sample position in the Dewar, minimizing the effects of the large axial stray fields on the spectropolarimeter. Photomultiplier tubes were heavily shielded from magnetic fields with a combination of Co-netic and Netic shielding manufactured by the Perfection Mica Co. (Bensenville, IL)<sup>22</sup> and were further removed from the center of the magnetic field by  $\sim 90$  cm. Samples were cooled to form a glass by using liquid helium from the cryostat reservoir, and depolarization of the light beam by the glass was determined by measuring the CD spectrum of a nickel tartarate solution placed before and after the sample. Glasses for which the depolarization was greater than 5% were not used. Sample temperatures were measured by a carbon glass resistor, mounted in the copper sample block  $\sim 1$  cm above the sample, and calibrated from 1.5 to 300 K by Cryogenic Calibrations (Pitchcott, Aylesbury, Buckinghamshire, U.K.). An Oxford Instruments DTC-2 temperature controller connected to a Rh/Fe resistor maintained the temperature for  $T > 4.2$  to  $\pm 0.05$  K. Temperatures below the  $\lambda$ -point of helium were achieved by pumping on liquid helium in the sample chamber; the temperature was maintained with an Oxford Instruments manostat. MCD intensity is reported in units of  $\text{L mol}^{-1} \text{cm}^{-1} \text{kG}^{-1}$ . All LTMCD spectra shown were obtained at a field of 50 kG. The CD instrument was calibrated with an aqueous solution of camphorsulfonic acid (50 mg/100 mL gave  $\Delta\epsilon_{290} = 2.40 \text{ M}^{-1} \text{cm}^{-1}$ ).

EPR spectra were obtained at  $\sim 9.27$  GHz at 77 K on a Bruker ER 200 D-SRC EPR spectrometer (operating at 100-kHz modulation, 10-mW incident power, and 12.5-G modulation amplitude, unless otherwise stated). Sample temperatures between 7 and 60 K were obtained at  $\sim 9.40$  GHz with an Air Products LTD-3-110 Heli-Tran liquid-helium transfer refrigerator and a Lake Shore Cryotronics, Inc., cryogenic temperature controller, Model DTC-500.

**LTMCD of Native Laccase.** In ref 13 we reported the temperature-dependent absorption and MCD spectra of native laccase at pH 6.0. The  $1/T$  dependence of the entire MCD spectrum (300–800 nm) indicates that the paramagnetic type 1 and type 2 copper centers in laccase have significant MCD contributions throughout this spectral region. Extension of these studies down to 1100 nm produces an additional broad feature associated with a paramagnetic ground state at  $\sim 865$  nm. Any temperature-independent and therefore diamagnetic transitions due to the type 3 centers are obscured by the intense temperature-dependent features. However, assignment of this LTMCD spectrum is still complicated by the fact that  $\sim 25\%$  of the type 3 centers in preparations of the native enzyme are reduced.<sup>12</sup> These sites can be oxidized by excess peroxide,<sup>12</sup>

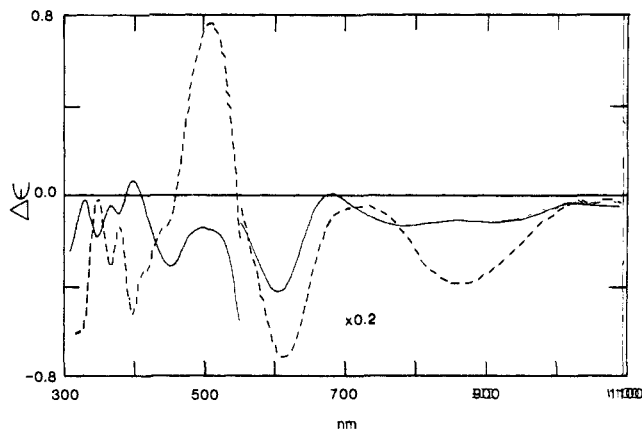


**Figure 2.** 4.8 K MCD spectra of reduced and oxidized type 3 laccase: (—) native laccase (pH 6.0) + 30 protein equiv of  $\text{H}_2\text{O}_2$  (oxidized type 3 center); (---) reduced type 3 laccase, estimated by removing the contribution of the 75% fully oxidized laccase to the pH 6.0 native laccase spectrum and correcting the concentration for 25% reduced type 3 centers in samples of native laccase at pH 6.0. [Protein] = 0.88 mM.

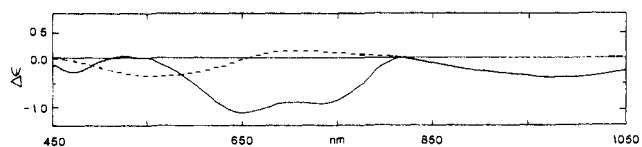


**Figure 3.** 4.2 K MCD spectra: (—) azurin (pH 7.4), adapted from ref 23; (---)  $[\text{Cu}^{\text{II}}\text{dien}]^{2+}$  at 5 K, pH 7.2, 50% (v/v)  $\text{Tris-SO}_4^{2-}$  buffer/glycerol.  $[\text{Cu}^{\text{II}}\text{dien}]^{2+} = 2.56 \text{ mM}$ . Although obtained at a slightly higher temperature than the azurin MCD spectrum, the intensity of the  $[\text{Cu}^{\text{II}}\text{dien}]^{2+}$  bands will increase  $\leq 10\%$  when  $T$  is lowered to 4.2 K, due to saturation effects.

and studies<sup>10</sup> of the T2D derivative have shown that the oxidation state of the type 3 center affects the spectral features of the type 1 center. Further, the anion-binding properties of the type 2 center in native laccase are a strong function of the oxidation state of the type 3 copper (vide infra), suggesting that the type 2  $\text{Cu}(\text{II})$  spectral features may also be affected by the oxidation state of the type 3 center. Thus, two sets of features can contribute to the LTMCD spectrum of native laccase (Figure 1): one from the type 1 and type 2 centers in the presence of an oxidized type 3 center and the second from the two paramagnetic centers in the 25% of the enzyme that contains reduced type 3 coppers. This spectrum is found to be strongly pH dependent over the range 4.6–7.0, as is also seen from Figure 1.

An LTMCD spectrum of fully oxidized laccase molecules (obtained by oxidizing with peroxide the reduced type 3 centers in preparations of native laccase) is presented in Figure 2 (solid line). Negative features occur at  $\sim 920$ , 780, 615, and 445 nm, with apparently several overlapping bands contributing to the 300–400-nm region. Most of these spectral features should be associated with the type 1  $\text{Cu}(\text{II})$  on the basis of a comparison with the LTMCD<sup>23</sup> and absorption<sup>24</sup> features of the  $\text{Cu}(\text{II})$  sites in azurin and plastocyanin, which are the blue copper sites most similar<sup>25</sup> spectroscopically to the type 1 center in laccase. The LTMCD spectrum of azurin in the 450–1050-nm region<sup>23</sup> is reproduced in Figure 3 (solid line). The negative 445-nm LTMCD band in native laccase appears to be related to the type 1 center as a band of similar sign and intensity is found in the 4.2 K MCD spectrum of azurin. This feature shows no strong pH dependence, does not undergo any major changes when the type 2 site binds  $\text{F}^-$  (vide infra), and is in the same spectral region as an imidazole  $\rightarrow \text{Cu}(\text{II})$  CT band found in plastocyanin.<sup>24,26</sup> The most intense feature of the fully oxidized native LTMCD spectrum is the negative band at 615 nm, which corresponds directly with the strong absorption band at this wavelength associated predominantly with cysteine  $\rightarrow \text{Cu}(\text{II})$  CT.<sup>24</sup> The 615-nm laccase ab-

(23) Greenwood, C.; Hill, B. C.; Barber, D.; Eglinton, D. G.; Thomson, A. J. *Biochem. J.* **1983**, *215*, 303–316.

(24) Solomon, E. I.; Hare, J. W.; Dooley, D. M.; Dawson, J. H.; Stephens, P. J.; Gray, H. B. *J. Am. Chem. Soc.* **1980**, *102*, 168–178.

(25) Spira, D. J.; Co, M. S.; Solomon, E. I.; Hodgson, K. O. *Biochem. Biophys. Res. Commun.* **1983**, *112*, 746–753.

(26) Solomon, E. I.; Gray, H. B. In *Copper Proteins*; Spiro, T. G., Ed.; Wiley-Interscience: New York, 1981; Chapter 1.

(22) Stephens, P. J., personal communication.

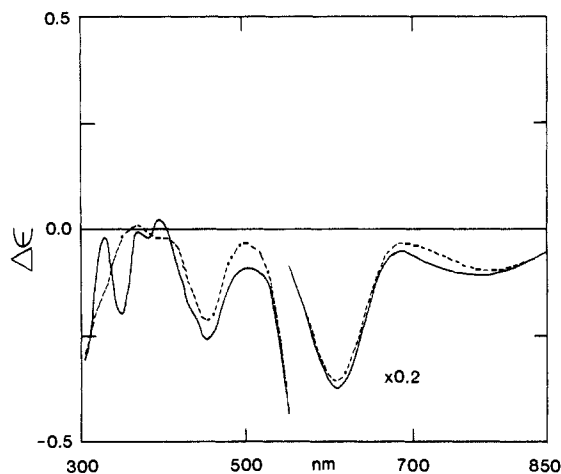


Figure 4. 4.2 K MCD spectra of native laccase (pH 6.0): (—) +30 protein equiv of  $\text{H}_2\text{O}_2$ ; (---) +25 protein equiv of  $\text{F}^-$  added to the peroxide-oxidized sample. [Protein] = 0.89 mM.

sorption band sharpens considerably on cooling<sup>13,27</sup> and is approximately 90% more intense than the corresponding absorption feature in azurin<sup>24</sup> at this temperature. As the intensity of an MCD band is expected to scale with the intensity of the corresponding absorption band,<sup>16</sup> this increase reasonably accounts for the greater LTMCD intensity of laccase at 615 nm when compared with the azurin LTMCD feature at 630 nm.

The 35 K absorption spectrum of azurin contains a band at 783 nm that has contributions from both a d-d and a CT transition. One of these components has a negative LTMCD feature at 725 nm. In laccase, an absorption band is found at 800 nm at 20 K<sup>27</sup> that appears to have a corresponding negative LTMCD feature at 780 nm. The similar intensity and energy of this band when compared with azurin indicate that it is likely associated with the type 1 center.

The remaining near-IR LTMCD feature at  $\sim 920$  nm cannot be confidently assigned. Although a negative LTMCD feature of similar intensity is found in the spectrum of azurin, its maximum occurs at significantly lower energy ( $\sim 1000$  nm). This indicates that an additional feature contributes to the LTMCD at this wavelength, which may be due to the type 2 center. The type 2 Cu(II) in oxidized laccase has been determined by EPR spectroscopy to have a tetragonal geometry and is expected to have weak contributions to the absorption spectrum in the 500–900-nm region due to ligand field transitions. Figure 3 (dashed line) shows the LTMCD of a tetragonal complex,  $[\text{Cu}^{\text{II}}\text{dien}]^{2+}$ , which contains three nitrogen ligands and a water molecule in a tetragonal geometry.<sup>28</sup> The features at  $\sim 550$  (negative) and 700 nm (positive) are associated with the d-d transitions of this molecule. From polarized absorption spectroscopy, Hathaway and Tomlinson have determined the assignment of the ligand field bands of tetragonal amine complexes<sup>29</sup> and have found that the  ${}^2E_g$  state lies highest in energy and is associated with the most intense part of the absorption spectrum. The 550-nm LTMCD feature of  $[\text{Cu}^{\text{II}}\text{dien}]^{2+}$  is reasonably associated with this  ${}^2B_{1g} \rightarrow {}^2E_g$  transition. The sign of this LTMCD band is also consistent with Kato's calculation of the C term associated with the higher energy spin-orbit component of the  ${}^2E_g$  state of  $[\text{Cu}(\text{NH}_3)_4]^{2+}$ .<sup>30</sup> These features will shift to lower energy as the complex becomes less square planar and more tetragonal. As seen in Figure 3, the LTMCD features of tetragonal Cu(II) are similar in magnitude to those of azurin in the 600–900-nm region; hence, it is difficult to distinguish features associated with the tetragonal type 2 center from those of the type 1 center. Anion-bound forms of oxidized laccase do not exhibit significant spectral perturbations in this energy region, which would have potentially allowed assignment of ligand field transitions. Thus, the type 2 ligand field features of the fully oxidized laccase LTMCD spectrum cannot be clearly distinguished from those of the type 1 Cu(II).

The type 2 Cu(II) should also contribute CT features to the LTMCD spectrum of oxidized laccase at higher energy. One CT transition associated with the type 2 copper can be identified by the addition of  $\text{F}^-$ ,

which binds to the type 2 Cu(II) of fully oxidized laccase and perturbs its CT spectrum (vide infra). The LTMCD spectrum of oxidized native laccase in the presence of 25 protein equiv of  $\text{F}^-$  is shown in Figure 4. At 345 nm, a negative feature found in the LTMCD spectrum of oxidized laccase (solid line) disappears upon binding of  $\text{F}^-$  (dashed line) and thus may be associated with a CT transition at the type 2 center. The intensity of this band does not appear to change over the pH range of 4.6–7.0, indicating that it is unlikely that the CT is from a protonatable ligand such as  $\text{OH}^-$ ; it is therefore reasonable to associate this with a protein-ligand  $\rightarrow$  (type 2) Cu(II) CT transition. The LTMCD spectrum of the tetragonal complex,  $[\text{Cu}^{\text{II}}(1,2\text{-Me}_2\text{Im})_4]^{2+}$ , shows a similar negative band at 320 nm.<sup>31</sup> The perturbation of the 345-nm laccase LTMCD feature upon binding  $\text{F}^-$  at the type 2 site also shows that the type 2 site can have a significant contribution to the absorption spectrum at this wavelength and thus should be at least partially responsible for the sharpening of the 298 K 330-nm absorption feature upon binding  $\text{F}^-$  (vide infra; Figure 13).<sup>17</sup>

The second set of spectral features present in the LTMCD spectrum of native laccase (Figure 1) are due to those molecules that contain a reduced type 3 center. X-ray absorption edge studies<sup>12</sup> demonstrate that approximately 75% of the protein molecules in native laccase in 0.1 M potassium phosphate buffer at pH 6.0 are fully oxidized. Thus, subtraction of 75% of the LTMCD intensity of fully oxidized native laccase (Figure 2, solid line) from the spectrum of native laccase at pH 6.0 (followed by normalization) allows an estimation of the LTMCD spectrum of the laccase molecules containing a reduced type 3 center (Figure 2, dashed line). Significant differences are found throughout most of the spectrum. In the ligand field region, a single broad negative band with increased intensity is observed at  $\sim 870$  nm, in contrast to the two negative features found in the spectrum of fully oxidized laccase. The large negative feature at 620 nm is slightly red-shifted upon type 3 reduction and  $\sim 75\%$  more intense, and a new positive feature appears at 510 nm. In addition, the negative band at 445 nm associated with the type 1 site of oxidized laccase appears to be absent, although this may be due to overlap with the relatively intense positive 510-nm feature. These changes indicate that reduction of the type 3 coppers strongly perturbs the electronic structures of the type 1 and the type 2 centers. It has already been observed through resonance Raman spectroscopy that changing the oxidation state of the type 3 center causes a structural change in the type 1 center in T2D laccase.<sup>10</sup> Alternatively, assignment of any new LTMCD features observed upon type 3 reduction to the type 2 Cu(II) would provide an important probe of the effects of oxidation state of the type 3 site on the geometric and electronic structure of the type 2 center.

The new features present in the LTMCD spectrum of reduced type 3 laccase can again be compared with the LTMCD spectrum of azurin (Figure 3). As several overlapping features are present in the 300–450-nm region, we do not attempt an assignment of this part of the spectrum. A weak positive feature at 525 nm in the LTMCD spectrum of azurin indicates that CT features associated with blue copper sites may have significant LTMCD intensity near this wavelength. However, considering the much greater intensity of the positive 510-nm feature in reduced type 3 laccase compared to the band in azurin, it is possible that the type 2 Cu(II) has a large contribution at this wavelength. The intensity increase at 615 nm should be correlated with the corresponding change in the absorption spectrum in order to determine the contribution from the type 1 center. Addition of peroxide to native laccase causes the type 1 298 K absorption feature at 615 nm to decrease by  $\sim 250 \text{ M}^{-1} \text{ cm}^{-1}$ .<sup>12</sup> Estimating the percentage of reduced type 3 centers as  $\sim 25\%$  in native protein solutions, a value of  $6450 \text{ M}^{-1} \text{ cm}^{-1}$  is determined for  $\Delta\epsilon_{615}$  of the type 1 Cu(II) in the presence of a reduced type 3 center. This represents an increase of  $\sim 18\%$  in the type 1 absorption intensity at 615 nm. The corresponding LTMCD intensity increases by nearly 75%, however, indicating that the LTMCD intensity is not scaling with the absorption intensity of the type 1 site. Thus, it appears that a significant contribution from the type 2 center must be present at this wavelength. Comparison of the azurin and reduced type 3 laccase LTMCD spectra at 870 nm shows that azurin does not have a feature that reasonably corresponds to the negative band in the laccase derivative, the LTMCD intensity of the 870-nm band being considerably greater than that of any azurin feature in this spectral region. Alternatively, d-d transitions from the type 2 copper in reduced type 3 laccase could contribute to the LTMCD intensity at 870 nm.

As an aid to assignment of these features, the spectrum of the reduced type 3 form may be perturbed by the addition of small amounts of  $\text{N}_3^-$ . Analysis of the CT spectrum of laccase to be presented in the next section has determined that "high-affinity" azide binding occurs at the type 2 Cu(II) in the presence of a reduced type 3 center. Thus, the changes

(27) Dooley, D. M.; Rawlings, J.; Dawson, J. H.; Stephens, P. J.; Andreasson, L.-E.; Malmstrom, B. G.; Gray, H. B. *J. Am. Chem. Soc.* **1979**, *101*, 5038–5046.

(28) Eickman, N. C. Ph.D. Thesis, Massachusetts Institute of Technology, 1979.

(29) Hathaway, B. J.; Tomlinson, A. A. G. *Coord. Chem. Rev.* **1970**, *5*, 1–43.

(30) Kato, H. *Mol. Phys.* **1972**, *24*, 81–97.

(31) Gewirth, A.; Solomon, E. I., unpublished results.

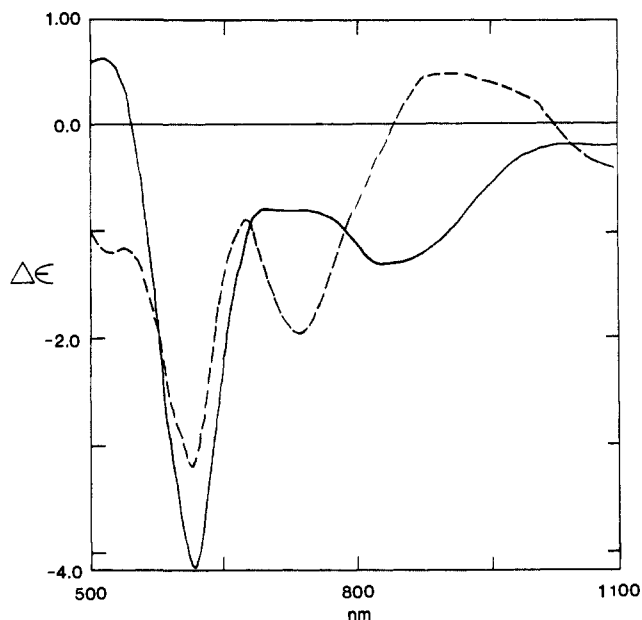


**Figure 5.** 4.9 K MCD spectra: (—) reduced type 3 laccase (pH 6.0); (---) reduced type 3 laccase + 0.5 protein equiv of  $N_3^-$ . [Protein] = 0.88 mM.

observed in the LTMCD spectrum upon binding of high-affinity  $N_3^-$  are expected to be dominantly associated with the type 2 Cu(II). Although changes in the 298 K absorption<sup>12</sup> and 15 K resonance Raman<sup>32</sup> of the type 1 Cu(II) are observed upon oxidation of the ~25% reduced type 3 molecules in laccase, significant changes are not observed upon  $N_3^-$  binding to native laccase,<sup>33</sup> indicating that the type 1 site is not strongly perturbed. While the spectral region at wavelengths shorter than 550 nm is obscured by  $N_3^- \rightarrow$  Cu(II) CT transitions (vide infra), changes do occur upon  $N_3^-$  binding at lower energies that may be associated with the d-d transitions of the type 2 copper center. Comparison of the LTMCD spectrum of the  $N_3^-$ -bound form of reduced type 3 laccase (Figure 5, dashed line) with that of reduced type 3 laccase in the absence of  $N_3^-$  (Figure 5, solid line) shows a positive change maximizing at ~620 nm accompanied by a negative band at ~725 nm. In addition, a loss of the negative 870-nm LTMCD band occurs, leaving a weaker positive feature centered at ~930 nm. The changes at ~620 and 870 nm are of similar magnitude and have the opposite sign of the intensity increases observed upon reduction of the type 3 center, indicating that negative bands at ~620 and 870 nm that grew in when the type 3 copper was reduced have shifted to other spectral regions upon binding  $N_3^-$  at the type 2 center. As these changes occur in the spectral region in which type 2 ligand field transitions are expected to be found, the negative bands at 620 and 870 nm are both reasonably assigned as d-d transitions of the type 2 site in reduced type 3 laccase. Although the direction and magnitude of the shift due to  $N_3^-$  binding are unclear due to the presence of the large  $N_3^- \rightarrow$  type 2 Cu(II) CT feature at ~510 nm and the inaccessibility of the spectral region to energies lower than 1100 nm, it is possible that one of these bands has moved to ~725 nm, where a negative feature appears upon binding  $N_3^-$ . The negative sign and high intensity of the 620- and 870-nm bands differ significantly from that found in tetragonal complexes (compare with Figure 3), indicating that the type 2 Cu(II) undergoes a strong distortion from tetragonal symmetry when the type 3 copper is reduced. Rivoal and Briat have shown that the sign and intensity of MCD C terms in Cu(II) are strongly dependent upon spin-orbit coupling of the ground and excited states with other excited states.<sup>34</sup> As the energy splitting of the Cu(II) ligand field excited states and the ground-state mixing changes with alterations in the coordination geometry, significant perturbations of the LTMCD spectrum of the type 2 Cu(II) are expected for large geometric distortions. Systematic studies on copper complexes will be required to define the nature of this distortion.

The strong pH dependence of the LTMCD spectrum of native laccase (Figure 1) can now be interpreted as primarily due to a pH-dependent equilibrium between laccase molecules containing reduced and oxidized type 3 centers. The LTMCD spectrum of fully oxidized laccase is es-

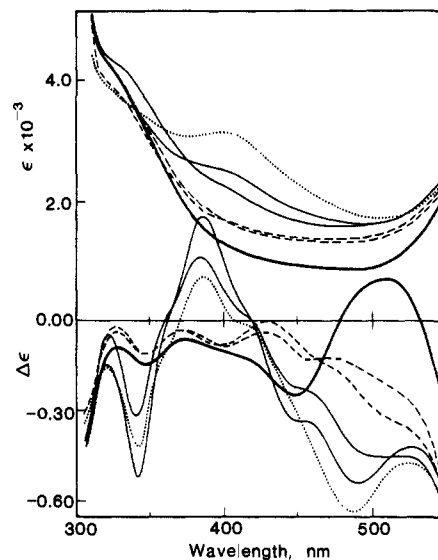


**Figure 6.** Titration of native laccase with  $N_3^-$ : upper, absorption (298 K) spectra; lower, LTMCD (4.9 K) spectra at 50 kG. Key: (bold solid line) native laccase; (---) 0.25 and 0.50 protein equiv of  $N_3^-$ ; (—) 2.5 and 9.0 protein equiv of  $N_3^-$ ; (···) 38.0 protein equiv of  $N_3^-$ .

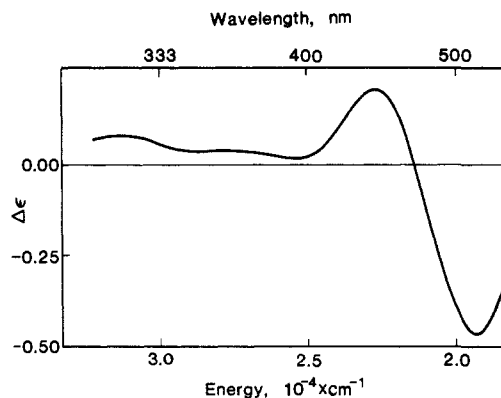


**Figure 7.** Difference LTMCD spectrum at 4.9 K of native laccase + 0.5 protein equiv of  $N_3^-$  (high affinity) relative to native laccase.

entially pH independent. When the pH of solutions of the native protein is lowered from 7.0 to 4.6, however, intensity increases are observed at 510 and 870 nm, where the type 2 Cu(II) in the presence of a reduced type 3 site contributes. The intensity increase observed at ~620 nm when the pH changes from 7.0 to 6.0 is similar to the increases at 510 and 870 nm. When the pH is lowered to 4.6, however, a slight intensity decrease is observed and the isosbestic point at 675 nm is lost. Thus, it appears that an additional form of the type 2 in the presence of a reduced type 3 center begins to contribute at low pH. The increase in reduced type 3 laccase upon lowering pH is consistent with studies of the pH dependence of high-affinity azide binding, results of which are presented in the next section.

**Azide Binding to Native Laccase.** When native laccase is titrated with azide, several sets of overlapping spectral features are observed (Figure 6: upper, absorption; lower, LTMCD) in the 550–300 nm region, which are assigned as  $N_3^- \rightarrow$  Cu(II) CT bands. These features have been described previously<sup>18,35</sup> as high-affinity azide binding ( $K > 10\,000\text{ M}^{-1}$ , dashed line) and low-affinity azide binding ( $K \sim 200\text{ M}^{-1}$  at 298 K, solid line). The intensities of the low-affinity features exhibit two types of behavior as a function of azide concentration. For azide concentrations  $\leq 9$  protein equiv, the intensity of the LTMCD bands increases continuously, following that of the absorption bands (solid lines). At higher azide concentrations (up to 38 protein equiv) dramatic decreases occur in some of the LTMCD features, while continuous intensity increases are observed for the absorption bands (dotted lines).

The binding of high-affinity azide produces a broad increase in the absorption spectrum between 400 and 500 nm:  $\Delta\epsilon_{410} = 630\text{ M}^{-1}\text{ cm}^{-1}$ ;  $\Delta\epsilon_{500} = 500\text{ M}^{-1}\text{ cm}^{-1}$  (Figure 6). In the corresponding difference

(32) Porras, A. G.; Spira, D. J.; Solomon, E. I., unpublished results.

(33) Thamann, T. J.; LuBien, C. D.; Solomon, E. I., unpublished results.

(34) Rivoal, J. C.; Briat, B. *Mol. Phys.* **1974**, *27*, 1081–1108.

(35) Morpurgo, L.; Rotilio, G.; Finazzi-Agro, A.; Mondovi, B. *Biochim. Biophys. Acta* **1974**, *336*, 324–328.

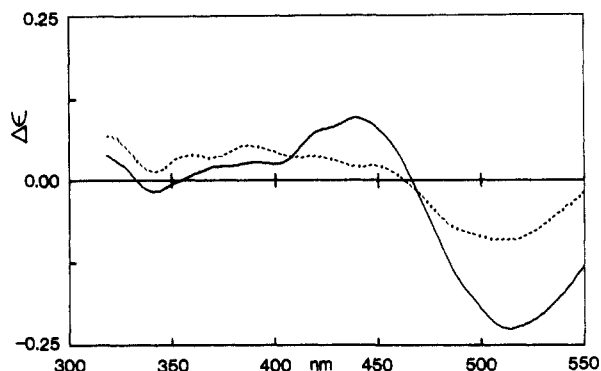


Figure 8. 4.9 K Difference MCD spectra: (—) pH 7.0 native laccase + 0.5 protein equiv of  $N_3^-$  (high-affinity  $N_3^-$  binding) and (---) the same sample with 30 protein equiv of  $H_2O_2$  added, relative to the spectrum of pH 7.0 native laccase. [Protein] = 0.81 mM.

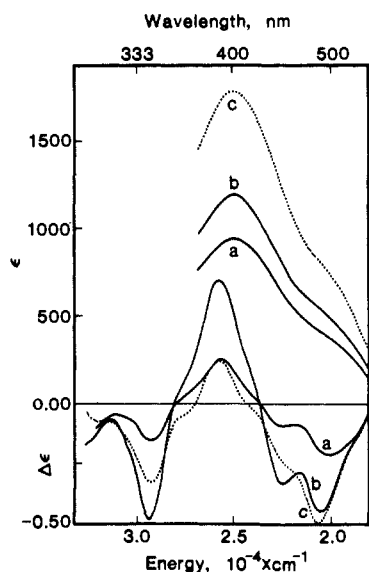


Figure 9. Low-affinity  $N_3^-$  spectral features: upper, absorption (298 K) difference spectra relative to an absorption base line with  $[N_3^-] = 0.5$  protein equiv (base-line variations at 77 K due to stray light and cracking of the sample glass preclude the calculation of accurate difference spectra at this temperature); lower, LTMCD (4.9 K) difference spectra at  $[N_3^-]$  of 2.5 (spectrum a), 9.0 (spectrum b), and 38.0 (spectrum c) protein equiv.

LTMCD spectrum (Figure 7) two bands of opposite sign are resolved at 510 and 445 nm. Since they are observed in the LTMCD spectrum, the ground state of the transitions must be paramagnetic; the bands are thus assigned to  $N_3^- \rightarrow$  (type 2) Cu(II) CT. These transitions have been assigned to the limited fraction ( $25 \pm 5\%$ ) of protein molecules in which the type 3 center is reduced.<sup>13</sup> The maximum intensity of the bands is obtained with less than 1.0 protein equiv of azide (0.5–0.75 protein equiv at [protein]  $\sim 1.0$  mM), and when laccase is oxidized with peroxide followed by addition of small amounts of azide, the intensities of the high-affinity absorption features are significantly reduced. Our LTMCD studies now confirm this assignment; Figure 8 shows the LTMCD difference spectrum of peroxide-oxidized laccase to which 0.5 protein equiv of  $N_3^-$  has been added (dashed line) compared with that of unoxidized native laccase plus 0.5 protein equiv of  $N_3^-$  (solid line). Both of these  $N_3^- \rightarrow$  Cu(II) CT bands decrease upon oxidation, indicating that they are associated with laccase molecules containing a reduced type 3 center. Similar results have also been demonstrated in EPR studies by Morpurgo et al.<sup>36</sup> We again note that comparison of the ligand field region of the LTMCD spectrum of reduced type 3 laccase (Figure 5, solid line) with that of the high-affinity  $N_3^-$  form (Figure 5, dashed line) shows that a significant geometric change of the type 2 center occurs upon binding azide.

(36) (a) Morpurgo, L.; Desideri, A.; Rotilio, G. *Biochem. J.* **1982**, *207*, 625–627. (b) Morpurgo, L.; Desideri, A.; Rotilio, G. In *The Coordination Chemistry of Metalloenzymes*; Bertini, I., Drago, R. S., Luchinat, C., Eds.; Reidel: Dordrecht, The Netherlands, 1983; pp 207–213.

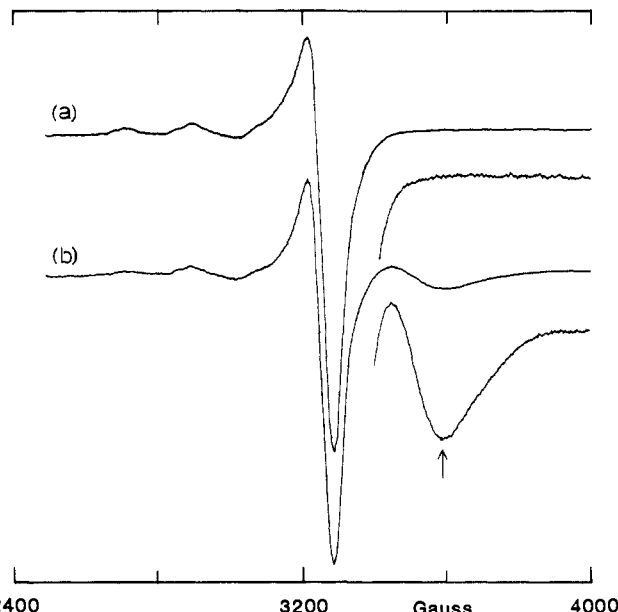


Figure 10. 8 K EPR spectra at 200-mW microwave power: native laccase (spectrum a); native laccase with 2.5 protein equiv of  $N_3^-$  (spectrum b). The high-field spectral region is shown at  $\sim 6\times$  higher gain, and the arrow points to  $g = 1.86$ .

The spectral features of low-affinity azide binding are shown in the difference spectra in Figure 9 in which the spectral contribution due to high-affinity azide has been removed. In the 298 K absorption spectrum (upper), a strong band at  $\sim 400$  nm with a broad shoulder extending to 500 nm is observed. Three sharp, negative bands at 340, 442, and 485 nm and an equally intense positive feature at 385 nm are observed in the corresponding LTMCD spectrum. The 485-nm LTMCD band corresponding to the absorption band at 500 nm indicates that the ground state of this transition is paramagnetic. Similar intensity behavior with increasing  $[N_3^-]$  is observed for both of these bands, showing that only one transition is involved. It is therefore assigned as a single  $N_3^- \rightarrow$  (type 2) Cu(II) CT transition.

The three remaining bands in the LTMCD spectrum exhibit much more complicated behavior. For  $[N_3^-] \leq 9$  protein equiv, the 340, 385, and 442 nm bands appear to grow in together (as indicated by the common crossover points at 351 and 422 nm) and to follow the intensity changes in the absorption spectrum. However, at higher  $[N_3^-]$  all three bands dramatically lose intensity, while the intensity of the absorption band at 400 nm continues to increase (Figure 9, dotted line). Thus, a simple correlation between the absorption and LTMCD features cannot be made.

In addition to the MCD and absorption features, a new signal is observed at  $g = 1.86$  in the EPR spectrum of low-affinity  $N_3^-$  at 8 K (Figure 10, arrow). This signal is characteristic of weakly interacting dipolar Cu(II) ions<sup>8</sup> and exhibits intensity changes with increasing  $[N_3^-]$  similar to those observed for the 340-, 385-, and 442-nm LTMCD bands. On the basis of its pH dependence and spectral shape, this EPR signal has been associated with a limited fraction of molecules in which  $N_3^-$  and  $H^+$  have competitively displaced and protonated the endogenous bridge,<sup>8,37</sup> thereby disrupting the antiferromagnetic coupling of the type 3 coppers. Since uncoupling the type 3 center renders it paramagnetic,  $N_3^- \rightarrow$  Cu(II) CT transitions due to  $N_3^-$  bound to this site will be observed in the LTMCD spectrum. The quantitative correlation observed<sup>13</sup> thus allows these three bands to be assigned to  $N_3^- \rightarrow$  (uncoupled type 3) Cu(II) CT transitions.

The lack of correlation of the 400-nm absorption band with the 385-nm LTMCD feature (Figure 9) indicates that an additional transition contributes to the absorption spectrum at 400 nm. An approximate magnitude for this band can be estimated by first determining the percentage of type 3 sites with bound  $N_3^-$  that are uncoupled, using the integrated EPR and the low-temperature binding constant for low-affinity  $N_3^-$  binding. If  $\epsilon$  of the additional feature is then estimated to be  $2500 \text{ M}^{-1} \text{ cm}^{-1}$  (a reasonable upper limit based on model copper–azide complexes),<sup>38</sup> then the additional feature comprises  $\geq 70\%$  of the absorption intensity at 400 nm but has no associated LTMCD intensity. Therefore,

(37) Wilcox, D. E.; Long, J. R.; Solomon, E. I. *J. Am. Chem. Soc.* **1984**, *106*, 2186–2194.

(38) Pate, J. E.; Solomon, E. I., unpublished results.

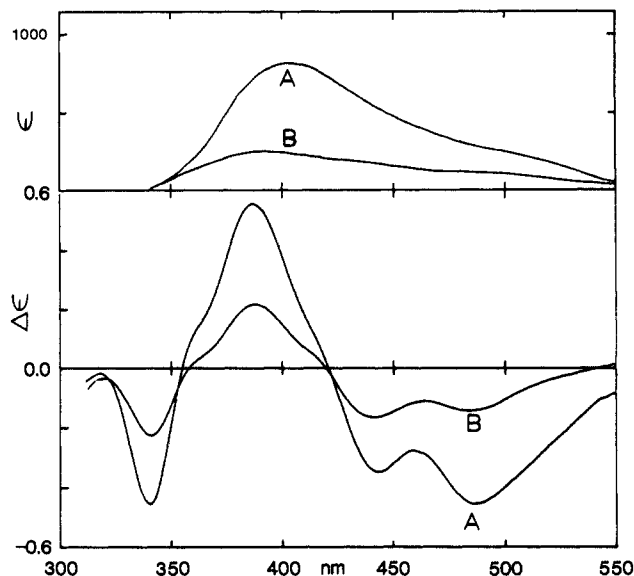


**Figure 11.** pH dependence on low-affinity  $N_3^-$  binding, relative to the high-affinity  $N_3^-$  base line (native + 0.5 equiv of  $N_3^-$ ): top, 298 K absorption; bottom, 4.9 K MCD spectra of native laccase + 9 protein equiv of  $N_3^-$ . [Protein] = 1 mM. Key: A, pH 6.0; B, pH 7.0.

the transition must arise from a diamagnetic Cu(II) center and can be assigned to an  $N_3^- \rightarrow$  (coupled type 3) Cu(II) CT transition. The behavior of this band when  $[N_3^-]$  is increased is qualitatively similar to that of the 485-nm LTMCD band (Figure 9), and the binding constants for the two bands are also similar.<sup>13</sup> Thus, both paramagnetic and diamagnetic CT transitions are produced by the binding of low-affinity  $N_3^-$ . There are two possibilities for azide binding that would produce this effect: either a single  $N_3^-$  bridges the type 2 and type 3 Cu(II) sites, or alternatively, two  $N_3^-$ 's with similar binding constants bind, one to the type 3 Cu(II) and one to the type 2 Cu(II) site.

Substantial evidence indicates that only one  $N_3^-$  is involved in low-affinity  $N_3^-$  binding, which must therefore be bound to both the type 2 and type 3 sites (see Discussion).<sup>13</sup> We report here two separate perturbations of  $N_3^-$  binding, in which both the 400-nm absorption and 485-nm LTMCD features are affected equally, indicating that only one azide is involved. The first of these perturbations is pH. It has been found that low-affinity  $N_3^-$  binding is inhibited by increasing the pH,<sup>18,35</sup> producing a large decrease in the intensity of the 400-nm absorption band. As shown in Figure 11, the intensity of the 485-nm LTMCD feature associated with  $N_3^- \rightarrow$  Cu(II) CT at the type 2 center as well as the 400-nm  $N_3^- \rightarrow$  (coupled type 3) Cu(II) CT absorption band is reduced by ~65% when the pH is raised from 6.0 to 7.0. This indicates that the pH change affects  $N_3^-$  bound to both the type 2 and type 3 sites equivalently, causing the amount of  $N_3^-$  bound at each center to decrease by the same amount. Such a similar pH effect is unlikely if the binuclear type 3 and the mononuclear type 2 centers were independently perturbed. This is further supported by the fact that the binding constant of the high-affinity  $N_3^-$  form to the type 2 site is not significantly affected by this change in pH ( $K = 31\,000\text{ M}^{-1}$  at pH 6.0 and  $29\,000\text{ M}^{-1}$  at pH 7.0, measured at 500 nm and 298 K).<sup>40b</sup> Thus, when the type 3 center is reduced, the pH effect is not observed at the type 2 Cu(II). This demonstrates that the oxidation state of the type 3 site strongly affects both the binding of anions by the type 2 and its pH behavior. Second, ligand competition studies of  $N_3^-$  with  $F^-$  (vide infra) show that  $F^-$  binding at the type 2 site directly competes with  $N_3^-$  binding at the type 3 site; the stoichiometry of the reaction eliminates the possibility of two  $F^-$ 's binding, one each at the type 2 and type 3 cupric sites. The combination of these results with the correlation of the 485-nm LTMCD and 400-nm absorption bands<sup>13</sup> shows that the spectral features of low-affinity  $N_3^-$  binding must be produced by a single azide molecule bridging the type 2 and type 3 cupric sites.

**Fluoride Binding to Native Laccase.** Addition of  $F^-$  to native laccase in 50% glycerol/0.2 M potassium phosphate buffer at pH 6.0 produces a superhyperfine doublet ( $I_F = 1/2$ ) of the type 2 Cu(II) EPR signal at 77 K (Figure 12B), increasing  $g_{\parallel}$  of the type 2 Cu(II) to 2.28 and decreasing its  $A_{\parallel}$  to  $166 \times 10^{-4}\text{ cm}^{-1}$ . The superhyperfine coupling constant of the doublets in the  $g_{\parallel}$  region of the type 2 Cu(II) is measured as  $66 \times 10^{-4}\text{ cm}^{-1}$  and requires equatorial coordination by a single  $F^-$  anion. Changes in the perpendicular region of the EPR spectrum are difficult to estimate accurately due to overlap with the type 1 features. Only at extremely high concentrations of  $F^-$  (~0.04 M) are traces of a triplet

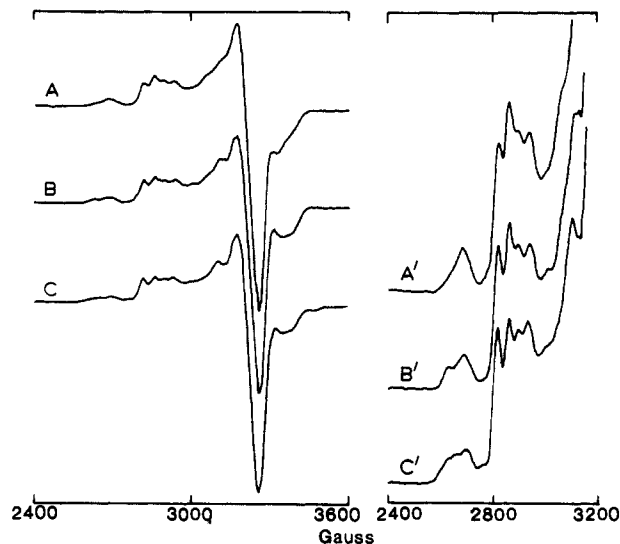


**Figure 12.** 77 K EPR spectra: (A) native laccase; (B) and (C) +1.0 and +38.0 protein equiv of  $F^-$  in 50% v/v glycerol/0.2 M potassium phosphate buffer, respectively. The primed spectra indicate the  $g_{\parallel}$  regions at ~6 $\times$  higher gain.

splitting observed in the EPR spectrum associated with a second  $F^-$  binding at the type 2 Cu(II) (Figure 12C). This indicates that the equilibrium binding constant for binding of a second  $F^-$  is  $\leq 10\text{ M}^{-1}$ . In the 298 K absorption spectrum,  $F^-$  binding in glycerol/phosphate buffer is characterized by an apparent sharpening of the 330-nm region, resulting in an absorbance decrease at 390 nm of  $400\text{ M}^{-1}\text{ cm}^{-1}$  and an increase at 320 nm of  $1000\text{ M}^{-1}\text{ cm}^{-1}$ , with an isosbestic point at 335 nm (Figure 13, top, dashed line). The MCD spectrum at ~5 K (Figure 13, bottom) shows small changes in the 550–300-nm region, the most significant of which occurs at 344 nm, where a negative feature in the LTMCD spectrum of the native enzyme (solid line) disappears upon addition of  $F^-$  (dashed line). This band is seen more clearly in the difference spectrum shown in Figure 13 (bottom, dotted line) and has been associated with the fully oxidized protein (Figure 4). The EPR (77 K), absorption (298 K), and MCD (5 K) features appear to maximize with ~1 protein equiv of  $F^-$ , consistent with an equilibrium binding constant of  $20\,000\text{--}40\,000\text{ M}^{-1}$ .

When 25 protein equiv of  $F^-$  is added to peroxide-oxidized native laccase, the changes observed in the LTMCD spectrum are essentially indistinguishable from those seen in Figure 13 (see Figure 4, LTMCD of Native Laccase section), indicating that these spectral changes are associated with the fully oxidized copper active sites, consistent with related EPR<sup>36</sup> studies. While the potential EPR spectral features associated with an additional  $F^-$  binding to the type 2 Cu(II) in the presence of a binuclear cuprous center would be weak and not easily observed (due to the relatively small concentration of enzyme molecules with a reduced type 3 center), the lack of competition between  $F^-$  and high-affinity  $N_3^-$  (see next section) demonstrates that  $F^-$  binds to the type 2 Cu(II) only in the presence of the oxidized type 3 pair.

In these results of  $F^-$  binding to native laccase, two significant differences are found in comparison with previous studies.

First, only a single  $F^-$  is observed to bind in protein solutions that contain glycerol, which is required in order to obtain an optical-quality, strain-free glass at low temperatures; earlier studies in 0.1 M potassium phosphate buffer, pH 6.0<sup>18</sup> and 5.5,<sup>39</sup> found that two  $F^-$  ions bind to the type 2 Cu(II) site, as evidenced by triplet superhyperfine splitting of the type 2 Cu(II) EPR spectrum at 77 K. The higher affinity  $F^-$  binds with  $K \sim 10\,000\text{ M}^{-1}$ , while the lower affinity  $F^-$  binds with  $K \sim 1000\text{ M}^{-1}$ .<sup>18</sup> The perturbations due to  $F^-$  of the absorption and 77 K EPR spectra of native laccase in 50% glycerol/phosphate buffer are similar to those observed in pure phosphate buffer<sup>39,40a</sup> for the binding of the higher affinity fluoride (the lower affinity fluoride only weakly perturbs the absorption spectrum associated with high-affinity fluoride), and the binding constants are similar. Thus, glycerol does not appear to significantly affect the binding properties of the first  $F^-$ . The difference in the fluoride-binding properties of laccase may be due to coordination of

(39) Malkin, R.; Malmstrom, B. G.; Vanngard, T. *FEBS Lett.* **1968**, *1*, 50.

(40) (a) Spira, D. J. Ph.D. Dissertation, Massachusetts Institute of Technology, 1985. (b) LuBien, C. D. Ph.D. Dissertation, Massachusetts Institute of Technology, 1982.

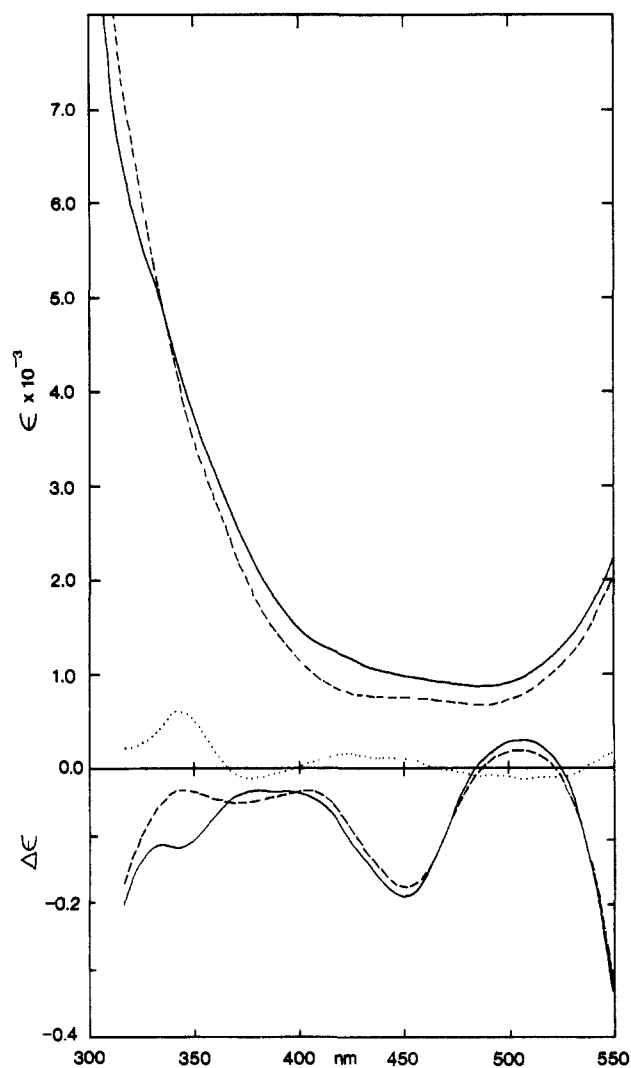


**Figure 13.** Spectra of native laccase + 1.0 protein equiv of  $F^-$ , pH 6.0, in 50% v/v glycerol/0.2 M potassium phosphate buffer: (—) native laccase; (---) +1.0 protein equiv of  $F^-$  ( $1.0 \times F^-$ ). Key: top, 298 K absorption spectrum; bottom, 5 K MCD spectrum; (· · ·) MCD difference spectrum ( $1.0 \times F^-$  - native laccase).

glycerol to one of the exchangeable positions at the type 2 Cu(II) (complexes of glycerol with copper are known<sup>41</sup>) or to a nonspecific effect of glycerol upon the tertiary structure of the protein.<sup>42</sup>

Second, EPR studies have shown that  $F^-$  binds to the type 2 site for  $T \leq 110$  K, but at 298 K, the superhyperfine splitting and  $g$ -value shifts found at low temperature are not observed.<sup>43</sup> This was interpreted to suggest that either  $F^-$  does not bind to native laccase at 298 K or it binds in a manner that does not affect the EPR spectrum. Studies of competitive binding between  $N_3^-$  and  $F^-$  from 298 down to  $\sim 5$  K to be presented in the next section show that these two anions compete and require a similar binding constant for  $F^-$  at all temperatures. The different EPR perturbations observed at room temperature and lower may thus be due to somewhat different modes of  $F^-$  binding, but the change in temperature does not appear (within experimental error) to significantly affect the equilibrium binding constants.

**Azide/Fluoride Competition in Native Laccase.** Our previous studies using absorption spectroscopy have reported<sup>18,44</sup> competitive binding by  $N_3^-$  and  $F^-$  at pH 6.0 to native laccase. Detailed elucidation of the competitive binding site was difficult, however, due to the multiple overlapping contributions to the absorption spectrum at the wavelengths

(41) Grun, A.; Bockisch, F. *Chem. Ber.* **1908**, *41*, 3465.

(42) Glycerol is found to have a significant effect upon the stability of proteins in solution and their folding mechanisms: Calhoun, D. B.; Englander, S. W. *Biochemistry* **1985**, *24*, 2095-2100.

(43) Morpurgo, L.; Agostinelli, E.; Senapa, M.; Desideri, A. *J. Inorg. Biochem.* **1985**, *24*, 1-8.

(44) LuBien, C. D. Ph.D. Dissertation, Massachusetts Institute of Technology, 1982.

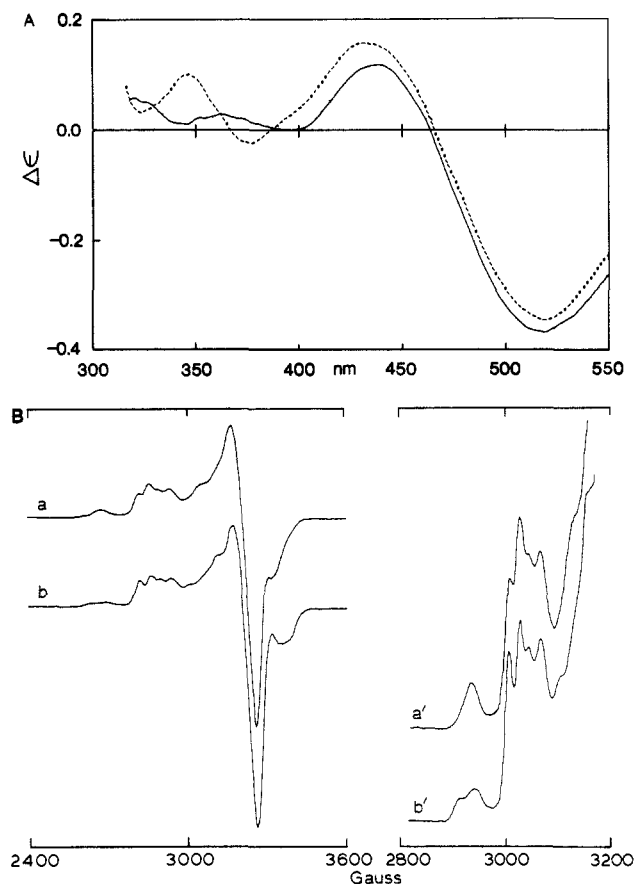


**Figure 14.** High-affinity  $N_3^-/F^-$  competition. (A) 4.9 K MCD difference spectra, relative to pH 6.0 native laccase: (—) 0.5 protein equiv ( $\equiv X$ )  $N_3^-$ ; (---)  $1.0 \times F^-$ ; (· · ·)  $0.5 \times N_3^- + 1 \times F^- - 0.5 \times N_3^-$ . [Protein] = 0.88 mM. (B) 77 K EPR spectra: (a) high-affinity azide; (b) sample in (a) after reaction with  $1.0 \times F^-$  (primed spectra recorded at  $\sim 6 \times$  higher gain).

of interest. This was further complicated by the incorrect presumption that peroxide was a ligand<sup>45</sup> and not simply an oxidant of the type 3 center.<sup>12</sup> This problem has now been resolved by the use of LTMCD combined with information obtained from the corresponding 77 K EPR, 298 K absorption, and X-ray absorption edge studies. Figure 14A (solid line) shows the LTMCD spectral changes that result when pH 6.0 laccase (in glycerol/phosphate buffer) reacts with 0.5 protein equiv of  $N_3^-$  ( $\sim 75\%$  high-affinity binding,  $\leq 5\%$  low-affinity binding). When 1.0 protein equiv of  $F^-$  is added to laccase equilibrated with 0.5 protein equiv of  $N_3^-$  (dashed line), the bands at 510 and 445 nm are essentially unaffected, although in the EPR spectrum a clear superhyperfine splitting of the lowest field type 2 hyperfine line and  $g_{\perp}$  peak at  $\sim 3350$  G (Figure 14B) is observed, indicating that  $F^-$  is bound to the type 2 site, as in native laccase in the absence of  $N_3^-$  (Figure 12). The small changes with  $F^-$  in the LTMCD spectrum are seen in the difference spectrum (Figure 14A, dotted line) and may be attributed entirely to  $F^-$  binding to type 2 sites on fully oxidized laccase molecules (compare with Figure 13,  $F^-$  section) and not to any displacement of high-affinity  $N_3^-$  by  $F^-$ . In particular, the positive change at 344 nm associated with  $F^-$  binding to oxidized native laccase is quite apparent (compare with Figure 4, LTMCD of Native Laccase section). This demonstrates that  $F^-$  binds only to oxidized laccase (see also Fluoride Binding to Native Laccase section).

LTMCD and 298 K absorption spectra are shown in Figure 15 for pH 6.0 laccase equilibrated with 9.0 protein equiv of  $N_3^-$  ( $\sim 50\%$  of the low-affinity  $N_3^-$  binding sites have  $N_3^-$  bound, with  $K = 200$   $M^{-1}$ ) before and after addition of 0.5-2.5 protein equiv of  $F^-$ . The intensity of the LTMCD features at 340, 385, and 442 nm associated with  $N_3^-$  bound to uncoupled type 3 Cu(II) centers, as well as the 485-nm LTMCD and 400-nm absorption bands associated with  $N_3^-$  binding to the type 2 and coupled type 3 Cu(II) centers, respectively, decreases dramatically as  $[F^-]$

(45) (a) Farver, O.; Goldberg, M.; Pecht, I. *Eur. J. Biochem.* **1980**, *104*, 71-77. (b) Farver, O.; Pecht, I. In *Copper Proteins*; Spiro, T. G., Ed.; Wiley-Interscience: New York, 1981; pp 152-218.



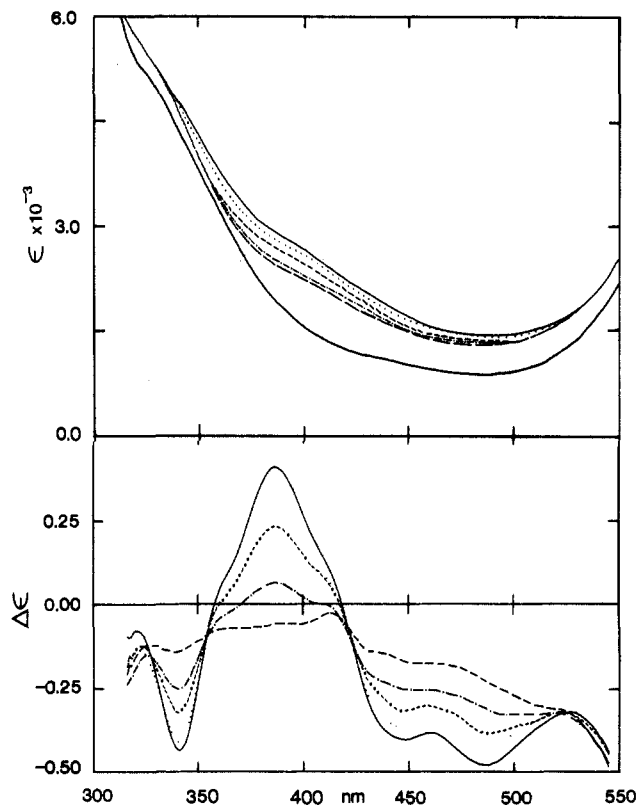


**Figure 15.** Low-affinity  $N_3^-/F^-$  competition: Top, 298 K absorption; bottom, 4.9 K MCD spectra of 9 protein equiv of  $N_3^-$  titrated with  $F^-$ . Lowest intensity curve in 298 K absorption data is native laccase, pH 6.0. Key: (—)  $9 \times N_3^-$ ; (⋯)  $+ 0.1 \times F^-$ ; (---)  $+ 0.2 \times F^-$ ; (- - -)  $0.5 \times F^-$ ; (long dashes)  $2.5 \times F^-$ . [Protein] = 0.66 mM.

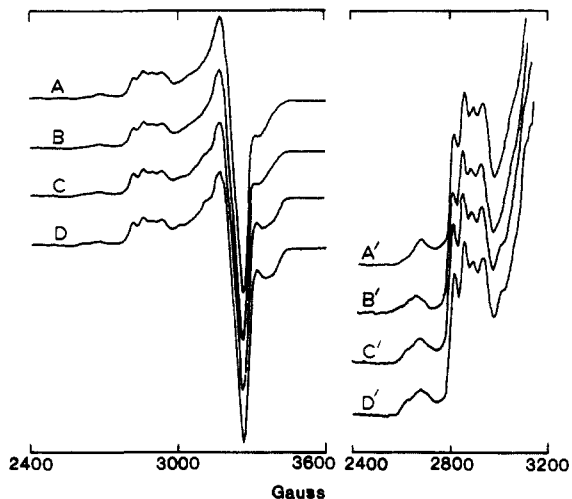


**Figure 16.** 77 K EPR spectra of low-affinity  $N_3^-/F^-$  competition: (A) native laccase reacted with 9 protein equiv of  $N_3^-$ ; (B)–(D) after reaction with 0.1, 0.5, and 2.5 protein equiv of  $F^-$ , respectively. The primed spectra indicate the  $g_1$  at 6 $\times$  higher gain.

is increased, indicating that low-affinity  $N_3^-$  is being displaced. The EPR spectra at 77 K (Figure 16) show superhyperfine splitting that demonstrates that  $F^-$  binding to the type 2 Cu(II) is associated with the disappearance of the absorption and MCD  $N_3^- \rightarrow Cu(II)$  CT features. The intensity changes of the 400-nm absorption and 485-nm LTMCD bands with  $F^-$  are plotted in Figure 17 (the intensities were normalized to a value of 1.00 for 0.0 equiv of  $F^-$ ). The two bands (solid lines) clearly decrease at the same rate, indicating that  $F^-$  displaces  $N_3^-$  from the type 2 and type 3 centers with approximately the same equilibrium binding constant. In order to determine the number of  $F^-$  ions involved in this competition, the amount of  $N_3^-$  displaced at a given  $[F^-]$  was calculated by using experimental equilibrium binding constants observed in the absence of competing ligand. If  $N_3^-$  and  $F^-$  compete for  $n$  binding sites in which the binding constant for each anion is the same at all sites, the

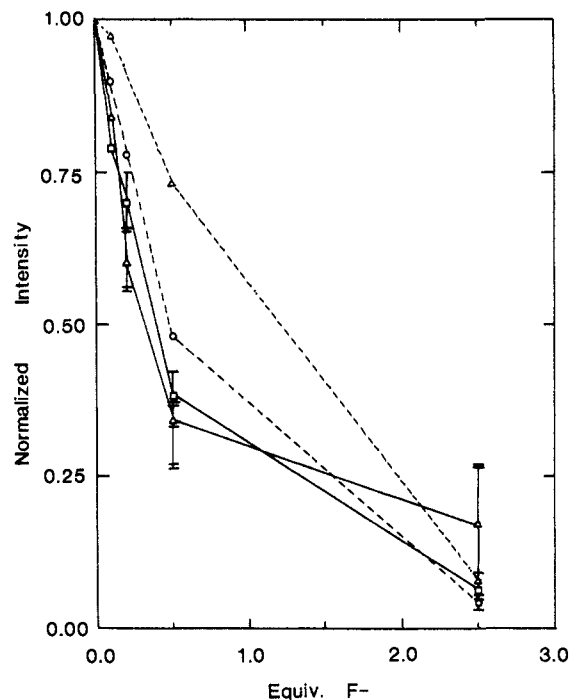


**Figure 17.** Correlation of 485-nm LTMCD and 400-nm 298 K absorption bands with theoretical curves for competition at 1 and 2 sites: (□–□) 485-nm LTMCD band; (Δ–Δ) 400-nm absorption band; (○–○)  $n = 1$ ; (Δ–Δ)  $n = 2$ . Intensities normalized to 1.00 at 0.0 protein equiv of  $F^-$  added. Error bars with double hatchmarks correspond to the 400-nm absorption band.

equilibrium concentration of bound  $F^-$  ( $[EF^-]$ ) may be calculated from eq 1,<sup>46,47</sup> where  $E_0$  = total protein concentration and  $K_F$  and  $K_{N_3^-}$  are the

$$[EF^-]/E_0 = nK_F[F^-]/[1 + K_F[F^-] + K_{N_3^-}[N_3^-]] \quad (1)$$

equilibrium binding constants for  $F^-$  and  $N_3^-$ , respectively. These equations neglect interactions between successively bound anions, so that each binding site is treated as independent of the other. We make the approximation that

$$[N_3^-] = [N_3^-]_0 - [EN_3^-] \sim [N_3^-]_0 \quad (1a)$$

since  $[N_3^-] \gg [EN_3^-]$  ( $[N_3^-]_0$  and  $[EN_3^-]$  are the amount of  $N_3^-$  added to the solution and the concentration of bound  $N_3^-$ , respectively). Making this substitution and rearranging, we obtain eq 2. An equation similar  $K_F[EF^-]^2 - [EF^-](1 + K_F[F^-]_0 + K_{N_3^-}[N_3^-]_0 + nE_0K_F) + nE_0K_F[F^-]_0 = 0$  (2)

to (1) obtains for the concentration of enzyme-bound  $N_3^-$ . The ratio as expressed in eq 3 is obtained from eq 1 and its counterpart for  $[EN_3^-]$ .

$$[EN_3^-]/[EF^-] = K_{N_3^-}[N_3^-]_0/[K_F([F^-]_0 - [EF^-])] \quad (3)$$

We now have two equations (eq 1 and 3) and two unknowns ( $[EN_3^-]$  and  $[EF^-]$ ). The error involved in making approximation 1a may be minimized by choosing a value of  $[N_3^-]$  that is the average of the amount of free  $N_3^-$  in solution when  $[F^-] = 0$  and the amount free when  $[F^-] = 2.5$  protein equiv. The independently determined binding constants used for  $F^-$  and low-affinity  $N_3^-$  are 40 000 and 200  $M^{-1}$ , respectively.

Table I shows values for  $[EN_3^-]$  calculated for two cases: if  $n = 1$ , then  $N_3^-$  and  $F^-$  compete at only one binding site, which must be the type 2 Cu(II) center since the EPR spectrum shows that this is where  $F^-$  binds (vide supra); if  $n = 2$ , then  $N_3^-$  and  $F^-$  compete independently at both the type 2 and the type 3 Cu(II) centers, with each  $N_3^-$  and  $F^-$  having the same binding constant at both centers. The values of  $[EN_3^-]$  are normalized to  $[EN_3^-]_0$ , which is the concentration of bound  $N_3^-$  before the addition of  $F^-$ . The calculated values may then be compared with those derived experimentally by using the 400-nm absorption feature as a probe of  $N_3^-$  binding to the type 3 center and the 485-nm LTMCD band as a probe of  $N_3^-$  binding at the type 2 center.  $\Delta\epsilon_{400}^0$  is the intensity of the  $N_3^- \rightarrow Cu(II)$  CT band observed at 400 nm in the 298 K ab-

(46) Steinhardt, J.; Reynolds, J. A. *Multiple Equilibria in Proteins*; Academic: New York, 1969.

(47) Klotz, I. M.; Triwush, H.; Walker, F. M. *J. Am. Chem. Soc.* **1948**, *70*, 2935–2941.

Table I. Calculated and Experimental Values for Enzyme-Bound  $N_3^-$ <sup>a</sup>

$[F^-]_0$	calculated		experimental	
	$[EN_3^-]/[EN_3^-]_0$ ( $n = 1$ )	$[EN_3^-]/[EN_3^-]_0$ ( $n = 2$ )	$\Delta\epsilon_{400}/\Delta\epsilon_{400}^0$	$\Delta(\Delta\epsilon_{485})/\Delta(\Delta\epsilon_{485})^0$
0.00	1.000	1.000	1.00	1.00
0.0655	0.899	0.976	$0.84 \pm 0.02$	$0.79 \pm 0.05$
0.131	0.787	0.913	$0.60 \pm 0.05$	$0.70 \pm 0.05$
0.328	0.481	0.729	$0.34 \pm 0.08$	$0.38 \pm 0.04$
1.64	0.045	0.074	$0.17 \pm 0.10$	$0.06 \pm 0.03$

<sup>a</sup> Enzyme concentrations are given in millimoles/liter.  $[\text{Protein}] = 0.512 \text{ mM}$  (corrected for 20% reduced type 3 centers).  $[N_3^-]_{\text{free}} = 5.65 \text{ mM}$ .

sorption spectrum in the absence of  $F^-$ , and  $\Delta\epsilon_{400}$  is the intensity of this band in the presence of various concentrations of  $F^-$ . Likewise,  $\Delta\epsilon_{485}^0$  is the intensity of the  $N_3^- \rightarrow \text{Cu(II)}$  CT band observed at 485 nm in the 5 K LTMCD spectrum in the absence of  $F^-$ , and  $\Delta(\Delta\epsilon_{485})$  is the intensity of this band after equilibration with various concentrations of  $F^-$ .

These experimental values are shown in Table I and are plotted in Figure 17 (solid line) with the calculated curves (dashed line) for  $n = 1$  and  $n = 2$ . The experimental ratios calculated from these two bands are the same within experimental error for a given  $[F^-]$ , indicating that the  $N_3^-$  bound to the type 2 center is displaced to the same extent by  $F^-$  as  $N_3^-$  bound to the coupled type 3 center. A comparison of the experimental data with the theoretical values calculated for  $n = 1$  and 2 shows that the experimental values are quite similar to those for the case  $n = 1$  but are clearly much smaller than those expected for the case  $n = 2$ . This indicates that the experimentally observed decreases in the 400-nm absorption and 485-nm LTMCD bands with  $F^-$  are much larger than those expected for  $N_3^-$  and  $F^-$  competing at both the type 2 and type 3 centers with similar binding constants. For example, when  $[F^-]_0 = 0.328 \text{ mM}$  ( $\sim 0.5$  protein equiv), a decrease of  $\sim 60\%$  is observed in the 485-nm LTMCD and 400-nm absorption bands; competition at two equivalent sites permits only  $\sim 28\%$  reduction of these bands, demonstrating that at this  $[F^-]_0$  it is not possible on the basis of stoichiometry to effect the observed change if two  $N_3^-$  (and  $F^-$ ) ions bind, one to the type 3 center and one to the type 2 center, with similar binding constants. Therefore, since low-affinity  $N_3^-$  and  $F^-$  compete at only one binding site, but the low-affinity  $N_3^- \rightarrow \text{Cu(II)}$  CT features associated with both the type 3 and type 2 centers decrease when  $[F^-]$  is increased, these data require that the low-affinity  $N_3^-$  CT features be a result of a single  $N_3^-$  binding to and bridging between the type 2 and type 3 centers.

## Discussion

The combination of LTMCD, absorption, and EPR spectroscopies provides significant insight into the interactions of exogenous ligands at the multicopper active site in native laccase. Previous studies<sup>19,36a,48</sup> have suggested that the T2 and T3 sites may be located close together. Through the correlation of the 485-nm LTMCD feature with the 400-nm absorption feature, which has no corresponding LTMCD feature, low-affinity  $N_3^-$  has been demonstrated to bridge the paramagnetic type 2 and antiferromagnetically coupled type 3 cupric centers. While it was also possible that two  $N_3^-$ 's with similar binding constants produced these paramagnetic and diamagnetic  $N_3^- \rightarrow \text{Cu(II)}$  CT features, studies at high pH and the stoichiometry of  $N_3^-/F^-$  competition experiments together demonstrate that a single bridging  $N_3^-$  produces these spectral features. Importantly, (i) increasing the pH from 6.0 to 7.0 results in an  $\sim 65\%$  decrease in both the 485-nm LTMCD feature and the 400-nm absorption band, where the binding constant of high-affinity  $N_3^-$  is not significantly affected by this change in pH, and (ii) the intensities of the  $N_3^- \rightarrow \text{Cu(II)}$  CT transitions at both the type 2 and the type 3 Cu(II)'s decrease when one  $F^-$  binds at the type 2 center, demonstrating that only one  $N_3^-$  is involved in low-affinity binding. (While there is clear evidence only at 77 K for  $F^-$  binding at the T2 Cu(II), the similarity of both the unusually high  $F^-$  binding constants and the low affinity  $N_3^-/F^-$  competition at 77 and 298 K suggest that a single  $F^-$  also binds to the T2 Cu(II) at 298 K.) This type 2-type 3 trinuclear copper cluster site is also consistent with the observation that upon reduction of the type 3 center, considerable changes in the type 2 LTMCD spectral features are observed. These changes indicate that there is a strong dependence of the geometric and electronic structure of the type 2 Cu(II) on the

oxidation state of the type 3 center. In particular, reduction of the type 3 center appears to cause a significant distortion of the type 2 Cu(II) away from tetragonal geometry.

In further support of a type 2-type 3 copper active site model, our studies indicate that the type 3 copper is strongly involved in the exogenous ligand reactivity of the type 2 copper center. Consistent with earlier studies,<sup>13,18,35</sup> azide affinity at the type 2 Cu(II) increases by at least 1 order of magnitude upon reduction of the type 3 center. Further, the binding constant associated with low-affinity  $N_3^-$  binding to the fully oxidized molecule decreases with increasing pH, while the binding constant for the high-affinity form is essentially unaffected by pH, suggesting there is a different  $\text{OH}^-$  involvement at the type 2 Cu(II) dependent upon the oxidation state of the type 3. In contrast with aqueous Cu(II) chemistry,  $F^-$  binds to native laccase with remarkably high affinity. Like high-affinity  $N_3^-$ ,  $F^-$  binds at the type 2 Cu(II), but the lack of competition between high-affinity  $N_3^-$  and  $F^-$  indicates that the binding constant of  $F^-$  decreases by  $\geq 10^3$  when the type 3 site is reduced. Hence, the origins of these high-affinity interactions are different. This unusually high  $F^-$  affinity for fully oxidized laccase suggests that  $F^-$  binds through a very specific interaction with the type 2-type 3 copper active site. The high affinity of  $F^-$  for the type 2 center may thus be due to the highly charged environment of the type 3 Cu(II) site, or alternatively, to an unusual binding orientation, possibly involving a direct interaction with the type 3 center. Thus, there is clearly a strong interaction between the type 2 and type 3 copper centers that results in the observed reactivity of native laccase. Studies aimed toward the elucidation of the detailed nature of this interaction are currently in progress.

The presence of a type 3-type 2 trinuclear copper active site in laccase that is capable of binding and bridging small molecules (at least azide) suggests that a similar binding mode may be active in the irreversible binding and multielectron reduction of oxygen to water. This model would differ significantly from the one generally considered<sup>7a,45</sup> in which oxygen bridges the type 3 site in laccase in a  $\mu$ -1,2 geometry, similar to that for oxyhemocyanin and oxytyrosinase, and has no direct interaction with the type 2 Cu(II) center. However, extensive ligand-binding and competition studies<sup>8</sup> of T2D laccase have now determined that exogenous anions do not bridge the type 3 coppers, but rather coordinate equatorially to one of the copper centers. Further, while there have been reports of two-electron-reduced, peroxide level intermediates of laccase, the two stable laccase forms, peroxy-laccase<sup>45</sup> and peroxy-T2D<sup>49</sup> laccase (which would parallel oxyhemocyanin and oxytyrosinase), have now been shown through X-ray absorption edge studies<sup>12</sup> to involve oxidation of the type 3 center but not binding by peroxide.

Alternatively, this trinuclear copper cluster may contribute to oxygen reduction by providing rapid three-electron transfer that would irreversibly break the O-O bond. Significantly, this trinuclear unit provides an all inner-sphere pathway for electron transfer to the bridging small molecule. Redox studies<sup>50</sup> of tetragonal Cu(I) and Cu(II) coordination complexes indicate that,

(49) (a) Farver, O.; Frank, P.; Pecht, I. *Biochem. Biophys. Res. Commun.* **1982**, *108*, 273-278. (b) Frank, P.; Farver, O.; Pecht, I. *Inorg. Chim. Acta* **1984**, *91*, 81-88.

(50) (a) Endicott, J. F.; Kumar, K.; Ramasami, T.; Rotzinger, F. P. *Prog. Inorg. Chem.* **1983**, *30*, 141-187 and references therein. (b) Al-Shatti, N.; Segal, M. G.; Sykes, A. G. *J. Chem. Soc., Dalton Trans.* **1977**, 1766-1771 and references therein.

(48) (a) Branden, R.; Deinum, J. *FEBS Lett.* **1977**, *73*, 144. (b) Martin, C. T.; Morse, R. H.; Kanne, R. M.; Gray, H. B.; Malmstrom, B. G.; Chan, S. I. *Biochemistry* **1981**, *20*, 5147-5155.

in the presence of an appropriate bridging ligand, these complexes exhibit a strong preference for inner-sphere electron transfer ( $K_{i.s.}/K_{o.s.} > 1000$ ). Bridging  $\mu$ -1,2 peroxy binuclear cobalt(II) coordination chemistry further indicates the importance of inner-sphere electron transfer to oxygen reduction, where, in all complexes studied,<sup>51</sup> peroxide further reduces via a  $\mu$ -1,1 rearrangement to the hydroperoxide, which yields a pathway for inner-sphere electron transfer. However, blue copper centers are capable of rapid outer-sphere electron transfer,<sup>52</sup> and in reoxidation studies of fully reduced laccase, the type 1 and type 3 centers are reported<sup>53</sup> to rapidly reoxidize while the type 2 copper appears

to remain reduced; these rates of reoxidation are, however, not consistent with turnover kinetics.<sup>53</sup> Nonetheless, a three-electron-reduced oxygen intermediate has been observed,<sup>53,54</sup> and an alternative role for the type 2-type 3 site could be in stabilizing this intermediate through a delocalized inner-sphere superexchange pathway. It is now important to determine the contribution of this type 2-type 3 cluster with respect to oxygen reactivity at the multicopper oxidase active site.

**Acknowledgment.** We are grateful to the National Institutes of Health (Grant AM31450) for support of this research.

**Registry No.** Cu, 7440-50-8;  $N_3^-$ , 14343-69-2;  $F^-$ , 16984-48-8; laccase, 80498-15-3.

(51) (a) Mori, M.; Weil, J. A. *J. Am. Chem. Soc.* 1967, 89, 3732. (b) Davies, R.; Sykes, A. G. *J. Chem. Soc. A* 1968, 2840-2847.

(52) Wherland, S.; Holwerda, R. A.; Rosenberg, R. C.; Gray, H. B. *J. Am. Chem. Soc.* 1975, 97, 5260-5262.

(53) Andreasson, L.-E.; Branden, R.; Reinhammar, B. *Biochim. Biophys. Acta* 1976, 438, 370-379.

(54) (a) Andreasson, L.-E.; Reinhammar, B. *Biochim. Biophys. Acta* 1979, 568, 145-156. (b) Aasa, R.; Branden, R.; Deinum, J.; Malmstrom, B. G.; Reinhammar, B.; Vanngard, T. *FEBS Lett.* 1976, 61, 115-119.

## Direct Observation by $^1H$ NMR of Cephalosporoate Intermediates in Aqueous Solution during the Hydrazinolysis and $\beta$ -Lactamase-Catalyzed Hydrolysis of Cephalosporins with 3' Leaving Groups: Kinetics and Equilibria of the 3' Elimination Reaction

R. F. Pratt\* and W. Stephen Faraci

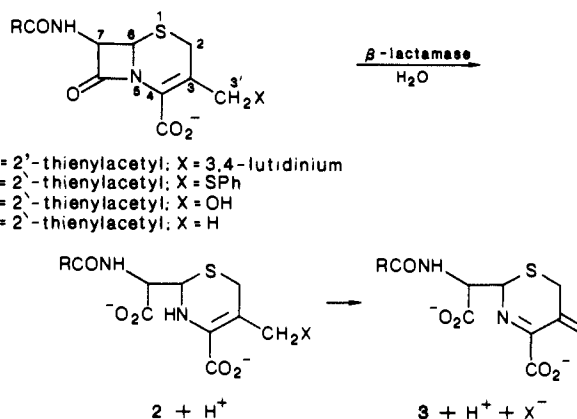
Contribution from the Department of Chemistry, Wesleyan University, Middletown, Connecticut 06457. Received January 31, 1986

**Abstract:** The hydrolyses of 3,4-dimethylcephaloridine, thiophenoxycephalothin, and desacetylcephalothin, catalyzed by the  $\beta$ -lactamases of *Enterobacter cloacae* P99 and the TEM-2 plasmid, yield cephalosporoate intermediates in solution that retain the 3' substituent. These intermediates have been characterized by their UV absorption and  $^1H$  NMR spectra. The 3' substituents, 3,4-lutidine, thiophenoxy, and hydroxyl, respectively, are then eliminated in a reaction, which is not enzyme-catalyzed, to give the well-known 5-exo-methylene-1,3-thiazine as final product. The elimination of 3,4-lutidine and thiophenoxy occurs rapidly and spontaneously but is also hydroxide ion catalyzed; phosphate buffer catalysis was not observed. On the other hand, the elimination of hydroxide ion from the other cephalosporoate is much slower and catalyzed by protons, hydroxide ions, and phosphate buffer. The elimination of 3,4-lutidine, pyridine (from cephaloridine), and thiophenoxy proceeds to a position of equilibrium, observable by  $^1H$  NMR. Analogous intermediates are generated on hydrazinolysis of these cephalosporins. Thus, the elimination of 3' leaving groups from cephalosporins is not, in general, concerted with nucleophilic  $\beta$ -lactam C-N bond cleavage.

The cephalosporins (**1**) are an important group of  $\beta$ -lactam antibiotics. Recently, we have provided evidence that, during the hydrolysis of cephalosporins with good 3' leaving groups, X, catalyzed by the RTEM-2  $\beta$ -lactamase, elimination of the leaving groups is not concerted with  $\beta$ -lactam cleavage.<sup>1</sup> An intermediate, whose absorption spectral characteristics were consistent with the structure **2**, was released by the enzyme, implying that the two-step reaction of Scheme I obtained. Preliminary observations of a similar nature have been reported by Page and co-workers.<sup>2</sup>

We have also shown that the elimination of the 3' leaving group can occur at a  $\beta$ -lactamase active site at the acyl-enzyme stage.<sup>3</sup> Subsequently, Grabowski et al.<sup>4</sup> showed, by direct  $^{13}C$  NMR observations, that intermediates analogous to **2** arise upon am-

Scheme I



(1) Faraci, W. S.; Pratt, R. F. *J. Am. Chem. Soc.* 1984, 106, 1489-1490.

(2) Agathocleous, D.; Buckwell, S.; Proctor, P.; Page, M. I. In *Recent Advances in the Chemistry of  $\beta$ -Lactam Antibiotics*; Brown, A. G., Roberts, S. M., Eds.; Royal Society of Chemistry: London, 1985; pp 18-31.

(3) Faraci, W. S.; Pratt, R. F. *Biochemistry* 1985, 24, 903-910.

(4) Grabowski, E. J. J.; Douglas, A. W.; Smith, G. B. *J. Am. Chem. Soc.* 1985, 107, 267-268.

monolysis of cephamycins in liquid ammonia at  $-50$  °C. Nevertheless, the structural identity of these intermediates has been questioned,<sup>5</sup> in our specific case and in general. This criticism